Solution Conformations of GM3 Gangliosides Containing Different Sialic Acid Residues As Revealed by NOE-Based Distance Mapping, Molecular Mechanics, and Molecular Dynamics Calculations†

Hans-Christian Siebert,‡,§ Gerd Reuter,§ Roland Schauer,§ Claus-Wilhelm von der Lieth,∥ and Janusz Dabrowski*,‡

Max-Planck-Institut für Medizinische Forschung, D-6900 Heidelberg, Germany, Biochemisches Institut, Christian-Albrechts-Universität, D-2300 Kiel, Germany, and Deutsches Krebsforschungszentrum, D-6900 Heidelberg, Germany

Received November 19, 1991; Revised Manuscript Received May 1, 1992

ABSTRACT: The conformation of the GM3 ganglioside, Neu5Acα2-3Galβ1-4Glcβ1-1Cer, and its analogs containing the Neu5Gc or Neu4Ac5Gc residues (Gc = glycolyl, CH_2OHCO) was investigated in Me_2SO-d_6 solution with the aid of a distance-mapping procedure based on rotating-frame NOE contacts, with hydroxyl protons being used as long-range sensors defining the distance constraints. A pronounced flexibility found for both the Neu-Gal and Gal-Glc linkages was confirmed by 1000-ps molecular dynamics simulations. Similar results, although based on a smaller number of NOE constraints, were obtained for GM3 gangliosides anchored in mixed D_2O/dodecylphosphocholine-d_{38} micelles and for the Neu5Ac-, Neu5Gc-, and Neu5,9Ac_2-sialyllactoses dissolved in D_2O. No noteworthy differences in conformational behavior of the glycan chains of the three gangliosides or sialyllactoses were observed in either of the media.

Gangliosides are sialic acid-containing glycosphingolipids that are ubiquitous components of mammalian plasma membranes. They play an important role in the interaction of cells with their environment and are thus involved in the regulation of many cellular events (Hakomori, 1990). The sialic acids found to date in gangliosides are *N*-acetyl-, *N*-glycolyl-, 9-*O*-acetyl-*N*-acetyl- and 4-*O*-acetyl-*N*-glycolylneuraminic acid (Reuter & Schauer, 1987).

N-Glycolylneuraminic acid (Neu5Gc) has frequently been detected in lower animals, probably starting in evolution with the echinoderms, and has also been found in many higher animals. In man, however, this sialic acid species is absent, except in tumors of the colon in which Neu5Gc-containing gangliosides are believed to represent tumor-associated antigens (Higashi et al., 1985). Furthermore, the presence of *N*-glycolylated sialic acids in sialo-glycoconjugates hinders the rapid degradation of these molecules by sialidases (Corfield & Schauer, 1982). The presence of a 4-*O*-acetyl-*N*-glycolyl group prevents the enzymatic release of this sialic acid (Schauer, 1979). These differences in comparison to Neu5Ac may possibly be due to conformational differences in the corresponding oligosaccharide chains.

The purpose of the present work was to investigate whether GM3[1] gangliosides containing different sialic acid residues differ in their conformational behavior. In particular, the extent of mobility of these residues was of considerable interest, since three conformations were observed for the NeuAc-Gal linkage in a terminal position in GM4 ganglioside (Poppe et al., 1989), whereas the same linkage located at the branch point in GM1 was shown to be fairly rigid (Acquotti et al., 1990).

Conformational studies of oligosaccharides using ^1H NMR spectroscopy mainly rely on the nuclear Overhauser effect (NOE), which reveals spatial proximities between protons (Noggle & Schirmer, 1971; Neuhaus & Williamson, 1989; Lemieux et al., 1980; Breg et al., 1980; Taravel & Vignon, 1982; Homans et al., 1982; Brisson & Carver, 1983; Paulsen et al., 1984; Koerner et al., 1984; Bush et al., 1986; Michon et al., 1987; Lipkind et al., 1989; Peters et al., 1990; Scarsdale et al., 1990; Sabesan et al., 1991a,b). The most severe drawback in such studies is the paucity of interproton contacts detectable by NOE. With, in the majority of cases, only one contact per glycosidic bond being observed, the conformation obtained is virtual (Jardetzky, 1980), i.e., it most probably refers to averaged interproton distances resulting from fast interconversion between different conformational states. This situation can be improved, however, if protons of hydroxy and amido groups are used as "long-range sensors" to provide additional contact information (Dabrowski & Poppe, 1989; Poppe et al., 1990a,b). Since NOE is inversely proportional to the sixth power of the internuclear distance, and since these protons protrude approximately twice as far as C-linked protons, many NOE contacts can be observed for each disaccharide segment of the oligosaccharide, and even for residues that are not directly linked to each other. In this way, the experimental basis for a verification of theoretically calculated conformation(s) can be greatly extended.

The calculations presented in this study were performed with use of the molecular mechanics MM2(85) program (Burkert & Allinger, 1982), with starting conformations obtained from purely geometrical analysis based on experimentally derived interatomic distances (Poppe et al., 1990a,b).

† Supported by the Deutsche Forschungsgemeinschaft and the Fritz Thyssen Stiftung.

* Author to whom correspondence should be addressed.
‡ Max-Planck-Institut für Medizinische Forschung.
§ Christian-Albrechts-Universität.
∥ Deutsches Krebsforschungszentrum.

[1] Abbreviations: NeuAc, *N*-acetylneuraminic acid; NeuGc, *N*-glycolylneuraminic acid; Gal, D-galactose; Glc, D-glucose; GalNAc, 2-acetamido-2-deoxy-D-galactose; Cer, ceramide; GM1, Galβ1-3GalNAcβ1-(NeuAcα2-3)4Galβ1-4Glcβ1-1Cer; GM3, NeuAcα2-3Galβ1-4Glcβ1-1Cer; GM4, NeuAcα2-3Galβ1-1Cer; GD1a, NeuAcα2-3Galβ1-3GalNAcβ1(NeuAcα2-3)4Galβ1-4Glcβ1-1Cer; SL, sialyllactose; DPC, dodecylphosphocholine; MM, molecular mechanics; MD, molecular dynamics; HSEA, hard-sphere exo-anomeric; CVFF, consistent valence force field; NMR, nuclear magnetic resonance; 1D and 2D, one and two dimensional; NOE, nuclear Overhauser enhancement; COSY, correlation spectroscopy; TQF, triple quantum filtered; TOCSY, total correlation spectroscopy; HOHAHA, homonuclear Hartmann–Hahn spectroscopy; RCT, relayed coherence transfer; ROESY, rotating-frame NOE spectroscopy; FID, free induction decay; TPPI, time-proportional phase increments; TORO, hybrid TOCSY–ROESY experiment.

0006-2960/92/0431-6962$03.00/0

The mobility of the monosaccharide units in the chain was simulated with the aid of the molecular dynamics (MD) program using the "consistent valence force field" (CVFF) introduced by Hagler et al. (1974, 1979).

The gangliosides were primarily examined in Me_2SO; this solvent enables one to observe sharp OH and NH resonances. In order to approach physiological conditions, however, Neu5Ac-GM3, Neu5Gc-GM3, and Neu4Ac5Gc-GM3 were also examined in D_2O in the form of mixed micelles with dodecylphosphocholine-d_{38} (DPC) (Eaton & Hakomori, 1988), and the saccharide parts (sialyllactoses) of the first two of these gangliosides, and also Neu5,9Ac_2 sialyllactose, were investigated in aqueous solution.

Unequivocal assignment of as many proton resonances as possible is a prerequisite for a reliable NOE-based structure determination. Because of the multiple signal overlap observed for these gangliosides in conventional two-dimensional (2D) correlated spectra (COSY), other techniques, namely, relayed coherence transfer (RCT) (Eich et al., 1982), triple quantum filtered (TQF) COSY (Piantini et al., 1982), and "total correlation" homonuclear Hartmann–Hahn spectroscopy (TOCSY; HOHAHA) (Müller & Ernst, 1980; Bax & Davis, 1985) were applied to achieve this goal. Both 1D and 2D NOE spectra were obtained in the rotating frame, in order to distinguish NOE signals from those due to exchange and to avoid any appreciable manifestation of spin diffusion. Overlapping NOE signals were deciphered with the aid of a hybrid TOCSY–ROESY experiment (Kessler et al., 1987; Poppe & Dabrowski, 1989).

MATERIALS AND METHODS

Neu5Gc-GM3 and Neu4Ac5Gc-GM3 gangliosides were extracted from horse blood (Veh et al., 1979). Neu5Ac-GM3 from human liver and Neu4Ac5Gc-GM3 were kindly provided by Dr. R. W. Veh, University of Bochum. Neu5,9Ac_2 sialyllactose was prepared from Neu5Ac sialyllactose (Ogura et al., 1987) and also isolated from rat urine (courtesy of Dr. T. J. Kornadt, University of Bochum). Deuterated solvents (D_2O and Me_2SO-d_6) and DCP-d_{38} were purchased from Merck, Sharp & Dohme.

Proton Nuclear Magnetic Resonance Spectroscopy. Prior to NMR measurements, the gangliosides were converted to their ammonium salts, dried in high vacuum, and dissolved in 0.35 mL of Me_2SO-d_6. Mixed micelles were prepared according to Eaton and Hakomori (1988) by dissolving the gangliosides and the detergent (molar ratio 1:40) in deuterated potassium phosphate buffer at p*D* 6. The mixture was exchanged twice with D_2O, with intermediate lyophilization, dried in high vacuum, and finally dissolved in 0.35 mL of D_2O. The oligosaccharide part of Neu5Gc-GM3, which was obtained from Neu5Gc-GM3 by ozonolysis (Wiegandt & Bücking, 1970), was also exchanged twice with D_2O, with intermediate lyophilization, dried, and dissolved in 0.35 mL of D_2O. Spectra were obtained at a frequency of 500 MHz on a Bruker AM-500 spectrometer equipped with an Aspect 3000 computer and a process controller. Chemical shifts were referenced to Me_4Si either directly (for micelles) or indirectly (for other solutions) by setting the ^1H signal of residual Me_2SO-d_5 to 2.50 ppm (at 300 K) or the signal of an added trace of Me_2CO to 2.225 ppm.

Two-dimensional COSY and RCT (Eich et al., 1982) spectra were recorded as previously described (Dabrowski, 1989, and references cited therein). Phase-sensitive 2D COSY, 2D HOHAHA, and 2D ROESY measurements were run in the TPPI mode (Marion & Wüthrich, 1983). For ROESY, the pulse sequence proposed by Rance (1987) was used, with a mixing (spin-lock) time composed of a train of short pulses (ca. 20° each), sandwiched between two z-filters with a delay of 3 ms and two 170° pulses (Dezheng et al., 1989). Additionally, a Hahn-echo pulse sequence was applied before acquisition (Davis, 1989), and the receiver phase was adjusted to the pure absorption mode in order to avoid baseline distortions (Marion & Bax, 1988). The carrier frequency was placed about 1.5 kHz downfield from the center of proton resonances during the mixing time but at the center during evolution and acquisition. The effective field for spin-locking was 2.5 kHz. A total of 512 free induction decays (FIDs), each of 32 scans, was accumulated with t_1 and t_2 acquisition times of 0.125 and 0.256 s, respectively. The relaxation delay was 1.2 s. The time–domain spectra were weighted in both dimensions with a squared sine-bell function shifted by $\pi/2$ and transformed to give a final resolution of 1.95 and 3.9 Hz/point in F_2 and F_1, respectively. Cross-peak volumes were calculated by using the standard Bruker 2D integration routine.

In order to assist the analysis of 2D spectra, some one-dimensional (1D) variants were also recorded, with the following experimental details. HOHAHA experiments were performed by selective excitation with a DANTE pulse sequence of 20–60 ms duration, followed by a MLEV-17 sequence for spin-lock and a z-filter in order to purge multiplet or phase distortions (Subramanian & Bax, 1987; Sorensen et al., 1984). In transient 1D ROESY experiments and DANTE pulse was followed by a train of short pulses of ca. 20°, and reference free induction decays (FIDs) were subtracted every eight scans. For the 1D hybrid TOCSY–ROESY (TORO) experiments (Kessler et al., 1987; Poppe & Dabrowski, 1989), the mixing interval was a combination of the two just described, and FIDs were subtracted every 16 scans.

Theoretical and Computational Aspects. These have been treated in detail in a previous paper (Poppe et al., 1990b), hence only the main points will be recapitulated here. Coexisting oligosaccharide conformers have never been directly observed in NMR spectra, hence these spectra must either represent a single rigid conformer or result from averaging on the NMR time scale. Since absolute rigidity of oligosaccharides can safely be excluded from consideration, the distances between two protons, H_k and H_l, determined by NOE (r_{kl}*), are in fact weighted averages of true distances (r_{kl}) between the same protons in different, mutually interconverting conformational states. These states may correspond to discrete conformers separated by an energy barrier or to different stages of an intramolecular rearrangement proceeding within *one* potential valley. For either of these two alternatives there must be at least one pair of true $H_k \cdots H_l$ distances, one of them being larger and the other smaller than the measured NOE distance, i.e., $r_{kl} < r_{kl}^* < r_{kl}'$. Our analysis concentrates on probing the conformational space within the $r < r^*$ distances, where at least one conformation certainly exists, and neglects the conformations with $r' > r^*$ (it may, however, be possible to define these other conformations given further NOE observations for other proton pairs). Since the main conformational feature of oligosaccharides, namely, the mutual orientation of every two monosaccharide units, is defined by the two glycosidic torsion angles Φ and Ψ, the encirclement of the conformational space by r_{kl}^* is performed in the Φ,Ψ coordinates to produce the familiar Ramachandran-type representation. The effective average positions of the protons of the pendent groups have been calculated and then taken into account in the distance-mapping procedure (Poppe et al., 1990a,b). The rotamer populations of pendent groups were

calculated on the basis of both NOE contacts with the neighboring C-linked protons and also vicinal coupling constants by taking the modified Karplus equations for hydroxyl (Fraser et al., 1968), amido (Bystrov et al., 1973), and hydroxymethyl (Haasnot et al., 1980) groups into account. The coupling constants were measured in conventional 1D spectra for well-separated signals and in 1D HOHAHA and/or 2D phase-sensitive COSY spectra in the case of signal overlap. The lower limit of the radius, r_{kl}(min), is taken to be equal to the sum of the van der Waals radii of the two relevant protons.

A single pair of contours drawn by r_{kl}* and r_{kl}(min) encircles an infinite number of possible combinations of the glycosidic torsion angles Φ and Ψ, in other words, it does not define any particular conformation. If, however, another pair of contours overlaps in a certain area with the former, it is likely that this area defines the geometry of the molecule in the Φ,Ψ space. Although it could be argued that r* determined for the other pair of protons refers in fact to a different Φ,Ψ combination and that the overlap is accidental, this possibility renders less and less likely with an increasing number of overlapping contours. It can be therefore concluded, with a high degree of confidence, that a mutliply overlapped areas defines a real conformation (cf. Figure 1) provided this conformation is within an energy-allowed region. We demarcate such regions in a similar fashion to the Ramachandran maps drawn for dipeptides (Cantor & Schimmel, 1980) but take into account (Poppe et al., 1990b) the relief of steric stress resulting from small variations of atomic positions, as first calculated for cellobiose and maltose (French, 1988; Tran et al., 1989).

The NOE distances r_{kl}* were obtained using the equation $r_{kl}^* = r_{ij}(V_{ij}/V_{kl})^{1/6}$, where V_{kl} and V_{ij} are the cross-peak volumes for the unknown and calibration distances, respectively, measured by the standard Bruker 2D integration routine from 2D ROESY spectra.

For molecular modeling, the oligosaccharides were constructed by successively attaching the appropriate monosaccharides with the use of the SUGAR program of the CARBHYD interface (von der Lieth et al., 1989). The coordinates for sugar ring atoms were taken from the Cambridge Crystallographic Data Bank. Substitution of the exocyclic groups was accomplished with the aid of the MOLBUILD interface (Liliefors, 1983). The ROTDIS program of the CARBHYD interface was then used to generate the distance maps for the glycosidic linkages. The Φ,Ψ angles defined by the areas of multiple overlap of the NOE distance contours, calculated from NOEs obtained for different proton pairs, were taken as starting values for the molecular mechanics (MM) calculations. These were run on an IBM 3090 computer with the use of the standard MM2(85) force field, employing Marshalls Parameters for the amide bond (Burkert & Allinger, 1982). The standard bond dipole approach was used to describe the electrostatic interactions. In order to evaluate the effect of the solvent on the conformation, each of the structures was minimized with use of four different values of the dielectric constant (ϵ = 1.5, 4, 8, and 80). Since neither the Φ,Ψ angles obtained nor the torsion angles for the pendent groups differed more than by 4°, only the results referring to vacuum (ϵ = 1.5) will be discussed. The structures representing an energy minimum were then taken as starting geometries for molecular dynamics (MD) calculations with use of the CVFF (Hagler et al., 1974) and the DISCOVER 2.5 program (Biosym Technologies, 10065 Barnes Canyon Road, San Diego, CA 92121). The input files for DISCOVER were prepared following the automatic charge and parameter assignment procedure of INSIGHT II/DISCOVER 2.5. All MD simulations were carried out at a temperature of 300 K. No additional forces or cutoffs were used. The equilibration time was 50 ps, and the total simulation time was 1000 ps.

As with MM minimization, the MD simulations were carried out with different dielectric constants (ϵ = 1.5, 8, and 80) for each of the starting structures. Since the resulting geometries and relative populations of the conformers were nearly identical, only the results referring to ϵ = 8 will be discussed.

In addition, two simulations with explicit inclusion of water were performed for the Neu5Acα2-3Galβ disaccharide with use of the SOAK option of INSIGHT II for the generation of the water box. The details were as follows. Water model: simple point charge (SPC), number of H_2O molecules 325; unit cell dimensions: a = 16.0 Å, b = 14.5 Å, c = 15.5 Å, angles $\alpha = \beta = \gamma = 90°$; cutoff of the nonbonded interactions: 12.0 Å (with the maximum distance between two atoms in the molecule 11.4 Å); equilibration time 50 ps at 300 K, and the molecules were in a thermal equilibrium at this temperature for the rest of the simulation; periodic boundary conditions were used, with time step 1 fs, regenerate the symmetry/periodic box every 20 steps, recompute neighbor list of residues every 20 steps, and history output frequency every 250 steps.

The generation of the various trajectories was done with the ANALYSIS option of INSIGHT II. The trajectories were plotted and examined with the program DISANA (own software). All MD calculations were run on a SG-IRIS-4D-120 GTX computer.

RESULTS AND DISCUSSION

Full assignments of the resonances of the C-, O-, and N-linked protons observed for Neu5Ac-GM3, Neu5Gc-GM3, and Neu4Ac5Gc-GM3 in Me_2SO-d_6 solution are given in Table I. The chemical shifts of Neu5Ac-GM3 are in good agreement with those reported by Koerner et al. (1983), except for the few indicated in a footnote to Table I. Vicinal H,H coupling constants that were helpful in establishing the conformations of exocyclic groups are presented in Table II. Coupling constants and temperature coefficients for the hydroxyl and amido proton resonances are gathered in Table III. The coupling constants were measured from standard 1D spectra for well-resolved signals and from 1D HOHAHA and 2D phase-sensitive COSY spectra in the crowded regions.

The following nonoverlapping intraresidue ROESY cross-peaks were available as standards for calibration distances, r_{ij} (Cambridge Crystallographic Data Bank distances in parentheses): N3ax/N3eq (1.78 Å), N4/N6 (2.52 Å; only for Neu4Ac5Gc-GM3), N3eq/N4 (2.53 Å for Neu5Ac- and Neu4Ac5Gc-GM3), II1/II3 (2.70 Å), and II3/II4 (2.47 Å). The r_{kl}* distances used for distance mapping (Table IV) and for the calculation of the side-chain conformation (Table V) are averages obtained with cross-peak volumes V_{ij} of all pertinent standard cross-peaks.

Conformations of Neu5Acα2-3Gal, Neu5Gcα2-3Gal, and Neu4Ac5Gcα2-3Gal Linkages. Several interresidue NOEs used as constraints for distance mapping (Table IV) refer to H8 of the glycerol side chain of the sialic acid residues; hence, the conformation of this chain will be analyzed first. The H6-C6-C7-H7 (Θ_1) and H7-C7-C8-H8 (Θ_2) torsion angles can be estimated on the basis of the vicinal coupling constants $^3J_{6,7}$ and $^3J_{7,8}$, respectively, by using a Karplus equation adapted for molecules containing electronegative substituents (Haasnot et al., 1980). Although four possible solutions for each ^3J are obtained during a 360° turn of a torsion angle,

Table I: Chemical Shifts (ppm from Me_4Si) Measured at 500 MHz for Solutions of GM3 Gangliosides[a] in Me_2SO-d_6 at 303 K

residue	proton	Neu5Ac-GM3 CH	Neu5Ac-GM3 OH(NH)[c]	Neu5Gc-GM3[b] CH	Neu5Gc-GM3[b] OH(NH)[c]	Neu4Ac5Gc-GM3 CH	Neu4Ac5Gc-GM3 OH(NH)[c]
Neuα-N	3ax	1.41		1.39		1.52	
	3eq	2.72		2.75		2.86	
	4	3.57	4.79	3.72	4.86	5.09	
	5	3.41	*8.03*[c]	3.46	*7.81*[c]	3.80	*7.73*[c]
	6	3.38[d]		3.50		3.71	
	7	3.19	4.57	3.21	4.55	3.25	4.37
	8	3.59[d]	6.14	3.60	6.20	3.57	6.01
	9a	3.37	4.18	3.34	4.21	3.35	4.21
	9b	3.62		3.63		3.57	
	10a			3.86	5.58	3.82	5.46
	10b			3.88		3.82	
	NAc	1.93					
	OAc					1.98	
Galβ-II	1	4.18		4.20		4.23	
	2	3.33	4.48	3.32	4.42	3.35	4.51
	3	3.97		3.98		3.93	
	4	3.70	4.44	3.70	4.42	3.72	4.38
	5	3.33		3.32		3.34	
	6a	3.44	4.67	3.45	4.67	3.48	4.65
	6b	3.46[d]		3.45		3.48	
Glcβ-I	1	4.16		4.16		4.16	
	2	3.02	5.11	3.04	5.11	3.04	5.11
	3	3.33	4.52	3.31	4.53	3.33	4.50
	4	3.28		3.30		3.28	
	5	3.28		3.27		3.30	
	6a	3.61	4.49	3.63	4.49	3.61	4.49
	6b	3.76		3.73		3.76	
Cer-C[e]	1a	3.39		3.40		3.39	
	1b	3.99		3.99		3.99	
	2	3.77	*7.50*[c]	3.76	*7.48*[c]	3.78	*7.50*[c]
	3	3.87	4.87	3.87	4.88	3.88	4.88
	4	5.37		5.34		5.36	
	5	5.54		5.54		5.54	
	6	1.94		1.96		1.92	

[a] For labeling, see formula in Figure 5. [b] The two C-linked protons of the *N*-glycolyl substituent are numbered 10a and 10b. [c] Italicized numbers refer to amido protons. [d] Koerner et al. (1983) reported δ(N6) 3.569, δ(N8) 3.40, and δ(II6b) 3.599. [e] Numbering for the ceramide residue: —$CH_2^{1a,b}$—CH^2[NHC(O)alkyl]—CH^3(OH)—CH^4=CH^5—CH_2^6—alkyl.

Table II: Vicinal Coupling Constants J (Hz) for Exocyclic Groups of GM3 Gangliosides in Me_2SO-d_6

compound	residue	^3J 5,6a	5,6b	6,7	7,8	8,9a	8,9b
Neu5Ac-GM3	Glc (I)	4.9	<2				
	Gal (II)	6.0	6.0				
	Neu (N)			2.3	9.9	6.2	*a*
Neu5Gc-GM3	Glc (I)	4.7	<2				
	Gal (II)	6.5	6.5				
	Neu (N)			2.2	8.7	5.8	2.8
Neu4Ac5Gc-GM3	Glc (I)	4.8	2.1				
	Gal (II)	6.5	6.5				
	Neu (N)			2.5	10.0	6.2	*a*

[a] Not determined because of signal overlap.

the correct one can be chosen by "NOE labeling", i.e., by establishing the spatial proximities of the vicinal protons to some other, firmly anchored protons. From the coupling constants and the intraresidue NOE distances given in Tables III and V, torsion angles were calculated as $\Theta_1 \approx -60°$ and $\Theta_2 \approx 180°$. This geometry appears to be stabilized by OH8 hydrogen bonding to the acceptor carboxylic group, as judged from the small $^3J_{H8,OH8}$ coupling constant (<2 vs ~6 Hz for a freely rotating OH8 group) and the small temperature shift coefficient of the OH8 resonance (Table III).

The conformations of the Neu-Gal linkages established by distance mapping turned out to be almost the same for all three of the GM3 gangliosides. The largest number of analyzable interresidue NOE contacts were obtained for Neu4Ac5Gcα2-3Gal (Table IV, cf. Table V); hence, its conformations determined by distance contours (Figure 1) are the best documented of the three. The areas of overlap for this ganglioside suggest three possible conformations with glycosidic angles Φ,Ψ around (1) –160°,–30°, (2) –80°,25° and (3) 100°,0°. The MM2-85 minimized conformations

Table III: Coupling Constants (Hz) and Temperature Coefficients k (-10^{-3} ppm/°C) for Amido and Hydroxy Protons of GM3 Gangliosides in Me_2SO-d_6

compd residue	proton	Neu5Ac-GM3 J	Neu5Gc-GM3 J	Neu4Ac5Gc-GM3 J	Neu4Ac5Gc-GM3 k
Glcβ (I)	OH2	3.5	3.6	4.1	5.8
	OH3	3.1	*a*	3.2	1.7
	OH6	5.7[b]	5.7[b]	5.4[b]	5.8
Galβ (II)	OH2	4.6	*c*	4.6	0.8
	OH4	5.0	*a*	6.2	5.0
	OH6	5.7[b]	5.0[b]	5.7[b]	4.2
Neuα (N)	OH4	5.6	5.5		
	OH7	3.0	3.5	4.5	4.2
	OH8	*c*	*c*	*c*	<2
	OH9	9.3[b]	*b*	8.2[b]	7.5
	NH5	7.2	7.2	8.7	5.8

[a] Not determined because of signal overlap. [b] Coupling constants for both methylene protons approximately equal. [c] Broadened, unstructured signal.

Table IV: Interresidual Contacts and Corresponding NOE Distances, r_{kl}*, for the GM3 Gangliosides

contacts		r_{kl}*	contacts		r_{kl}*
Neu5Acα2 → 3Galβ1 → 4Glc					
N3ax	II3	2.8	II1	I4	2.3
N3ax	II4	3.3	II1	I6a	3.2
N3eq	II4	3.4	II1	I6b	3.2
N8	II1	3.3	II1	IOH3	3.2
N8	II3	2.9	II1	IOH6	3.3
N8	II4	3.0	II6ab	IOH3	3.4
Neu5Gcα2 → 3Galβ1 → 4Glc					
N3ax	II3	2.8	II1	I4	2.3
N3ax	II4	3.1	II1	I6b	3.2
N8	II1	3.2	II1	IOH3	3.2
N8	II3	3.0	II1	IOH6	3.3
N8	II4	3.0	II6ab	IOH3	3.2
N8	IIOH2	3.0			
Neu4Ac5Gcα2 → 3Galβ1 → 4Glc					
N3ax	II3	2.8	II1	I4	2.3
N3ax	II4	3.3	II1	I6a	3.2
N3eq	II4	3.3	II1	I6b	3.2
N8	II1	3.3	II1	IOH3	3.2
N8	II3	2.9	II1	IOH6	3.4
N8	II4	3.2	II6ab	IOH3	3.2
N3ax	IIOH2	3.4			
N8	IIOH2	3.3			

Table V: Intraresidual Contacts and Corresponding NOE Distances, r_{kl}*, for Sialic Acid Residues of Neu5Ac-GM3, Neu5Gc-GM3, and Neu4Ac5Gc-GM3

Neu5Ac contacts		r_{kl}*	Neu5Gc contacts		r_{kl}*	Neu4Ac5Gc contacts		r_{kl}*
NNH	N4	2.5	NNH	N4	2.5	NNH	N4	2.6
NNH	N7	3.0	NNH	N7	3.1	NNH	N6	2.9
N5Ac	N7	3.0	N10ab	N7	3.0	NNH	N7	3.1
N5Ac	NOH7	3.3	N10ab	NOH7	3.4	N4Ac	N3eq	3.4
			N9a	N7	2.9	N4Ac	N5	3.2
			N8	NOH7	2.7	N4Ac	N10ab	3.3
						N4Ac	NOH10	3.2
						NNH	NOH7	3.2
						N6	N7	2.6

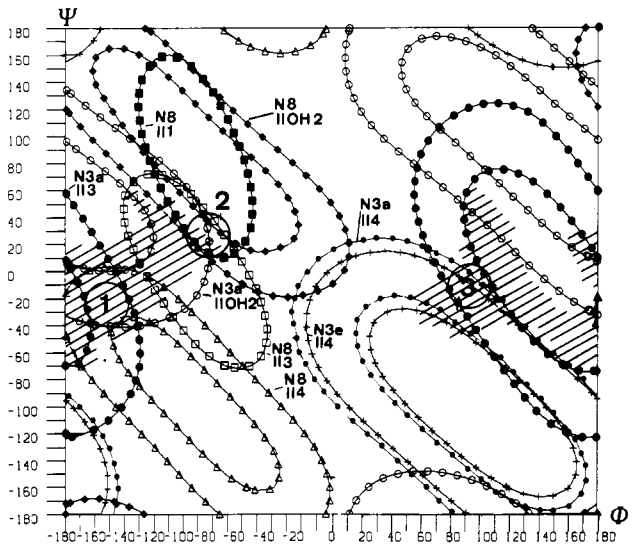

FIGURE 1: NOE and steric constraints for the Neu4Ac5Gcα2-3Gal linkage of the corresponding GM3 ganglioside (cf. Table IV). The labels at each pair of the contours refer to two protons showing a NOE contact; for labeling of these protons, see formula in Figure 5. Sterically allowed areas are hatched.

Table VI: Conformation of Neu5Acα2-3Galβ Segment in Various Moieties

compd	solvent	Φ,Ψ (°)			ref
GM3	Me_2SO	−161,−25;	−78,19;	84,34	this work
GM4	Me_2SO	−153,−26;	−85,12;	61,−14	Poppe et al. (1989)
a	D_2O	−160,−13			Sabesan et al. (1991a)
GM1[b]	D_2O	−165,−15			Sabesan et al. (1984)
GM1	Me_2SO	−165,−18			Acquotti et al. (1990)
GM1[c]	Me_2SO			85,61	Scarsdale et al. (1990)
GD1a[c,d]	Me_2SO			79,37	Scarsdale et al. (1990)
GD1a[b,d]	D_2O	−164,−19			Sabesan et al. (1991b)
e,f	D_2O	−160,−20	−70,5	−95,−45	Breg et al. (1989)
e,g	D_2O	−157,−22	−62,3[h]	−101,−56	Breg et al. (1989)
i	D_2O	−160,−15	−90,10	110,−20[j]	Bechtel et al. (1990)

[a] In Neu5Acα2-3Galβ1-O$(CH_2)_8CO_2$Me; almost identical Φ,Ψ values were obtained for five other oligosaccharides containing this terminal disaccharide segment. [b] Oligosaccharide released from the ganglioside. [c] Along with five almost identical conformations. [d] The internal Neu5Acα2-3Gal bond. [e] In Neu5Acα2-3Galβ1-4GlcNAcβ1-NAsn. [f] HSEA energy format. [g] MM2HB energy format. [h] Along with −64,−18. [i] In Neu5Acα2-3Galβ1(Fucα1-4) 4GlcNAcβ1-O$(CH_2)_8CO_2$Me; numerical Φ,Ψ values were read from an energy map. [j] Along with a high-energy 10,−90 conformation.

calculated with these starting geometries gave Φ,Ψ angles of (1) −161°,−25°, (2) −78°,19°, and (3) 84°,34°, i.e., only geometry 3 was markedly changed by the minimization procedure. It is interesting to compare these conformations with those found by other authors for terminal Neu5Acα2-3Gal disaccharide segments of various molecules (Table VI).

Thus, conformation 1 is practically the same as the only one found by several authors for terminal Neu5Ac residues in various oligosaccharides or branch Neu5Ac residues in GM1 and GD1a, and as one of three or four conformations reported for terminal Neu5Ac units in GM4, Neu5Acα2-3Galβ1-4GlcNAcβ1-NAsn and Neu5Acα2-3Galβ1-3(Fucα1-4)-GlcNAcβ1-O$(CH_2)_8CO_2$Me. Surprisingly, no similar conformation was found by Scarsdale et al. (1990) for either the branch or the terminal position of Neu5Ac in GM1, GM1b, and GD1a.

Conformation 2 is very similar to another, less populated conformation obtained for GM4 and to the most populated conformation reported by Breg et al. (1989) for the same terminal disaccharide segment of the asparagine sialyllactosamine. Sabesan et al. (1991b) discussed a possible existence of a somewhat similar conformation (−80°,−10°; along with the preferred conformation −163°,−12°) for the terminal Neu5Ac residue in GD1a, but in another work from the same laboratory this conformation has not been found in either of six oligosaccharides containing the terminal Neu5Acα2-3Galβ segment (Sabesan et al., 1991a). Veluraja and Rao (1983) obtained −67°,−7° for GM3 by empirical energy calculations and excluded a −155°,−20° conformation, for which the energy was 4 kcal/mol higher.

Conformation 3, which is not very precisely defined by distance mapping (Figure 1) and has the highest calculated energy, differs considerably from the third conformation of GM4 and bears no resemblance to any conformation of sialyllactosamine. Remarkably, it is nearly identical to the only conformation of the branch Neu5Acα2-3Gal segment of GM1 and GD1a reported by Scarsdale et al. (1990).

To test how real these three conformations of the Neu-Gal segment are, its dynamic conformational behavior was simulated with use of the MD DISCOVER program. MD calculations are capable, in principle, of reproducing the internal motions of a molecule and representing them in the form of variations with time of different structural parameters, e.g., internuclear distances or torsion angles (Karplus & McCammon, 1981; French & Brady, 1990). In this way, structures obtained on the basis of time-averaged NMR data, such as NOE and coupling constants, may be resolved into separate conformations that contribute to these "virtual" structures. Alternatively, as in the present work, the particular conformations determined experimentally, e.g., by distance mapping, may be verified by observing their behavior in a suitable force field (Dabrowski et al., 1990). As pointed out by de Vlieg and van Gunsteren (1991), no generally applicable force field exists at this time, and any potential energy function contains approximations that restricts its range of validity. Concerning oligosaccharides, the advisability to include a potential corresponding to the exoanomeric effect is problematic, since its excessively large energy requirement would certainly result in an overestimated rigidity of the structure (Tvaroska & Perez, 1986). Hence, it was of particular interest to use a force field developed for systems containing many structural elements similar to those present in oligosaccharides but not parameterized for exoanomeric effect. From this point of view, the DISCOVER program and its consistent valence force field designed first for peptides and further developed to include systems with a large "density" of hydrogen bonds (Hagler et al., 1974, 1979) seemed suitable as a first approximation. The fact that the simulations described below were in agreement with the conclusions based on extended sets of NOEs speaks of the transferability of the CVFF in this case and suggests that the role of the exoanomeric effect should be further examined by combining computational and effective experimental methods.

The MM-minimized Φ,Ψ angles of conformation 1 were used as input in the 1000-ps simulation shown in Figure 2a. The Φ,Ψ trajectories show that after a short period of equilibration, the molecule dwells during longer time intervals either in a geometry characterized by average values of $\Phi \approx -155°$ and $\Psi \approx -25°$ or alternatively in a conformation approximated by $\Phi \approx -75°$ and $\Psi \approx 10°$, showing only moderate fluctuations around these averages. In view of the many uncertainties involved in both the experimental and the computational methods, the small differences between these averages and the values obtained from distance maps for conformations 1 and 2 are of no concern. Most significantly,

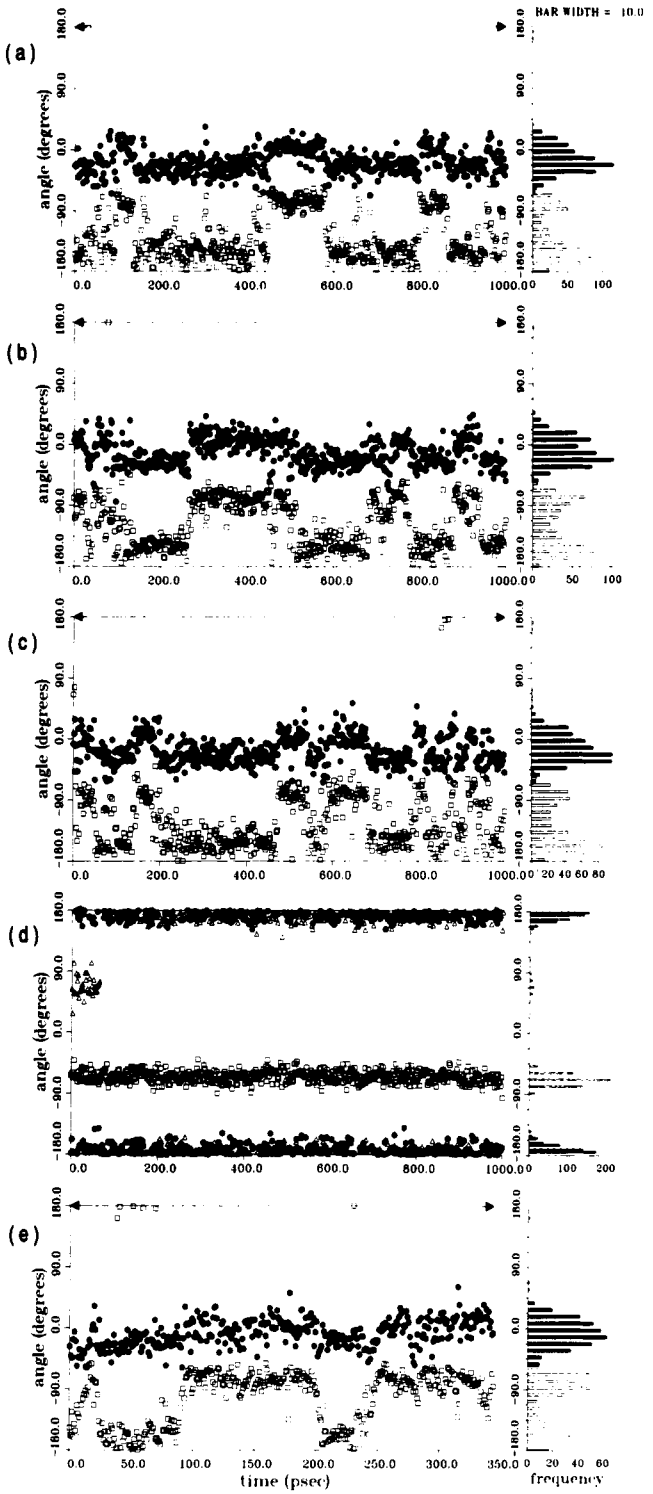

FIGURE 2: Histories of the glycosidic and side-chain torsion angles for the Neu5Gcα2-3Galβ disaccharide segment. (a), (b), (c): 1000-ps simulations referring to $\epsilon = 8$ (dielectric constant of the medium), started with input Φ(□),Ψ(●) values corresponding to conformations 1–3, respectively (cf. Figure 1). (d): A 1000-ps simulation for the H6-C6-C7-H7 (θ1) (□), H7-C7-C8-H8 (θ_2) (●), and H8-C8-C9-H9 (△) torsion angles. (e): As in panel a, but water molecules were explicitly included and the simulation was run for 350 ps.

the jumps between the Φ,Ψ values were synchronous in the vast majority of cases. These transitions were also reproduced, in a reverse order, by a simulation started from the geometry 2 (Figure 2b). Neither this nor the first simulation gave evidence for the existence of conformation 3. In keeping with this, the Φ,Ψ trajectories did not halt at the input values in a simulation started from this conformation (Figure 2c) but

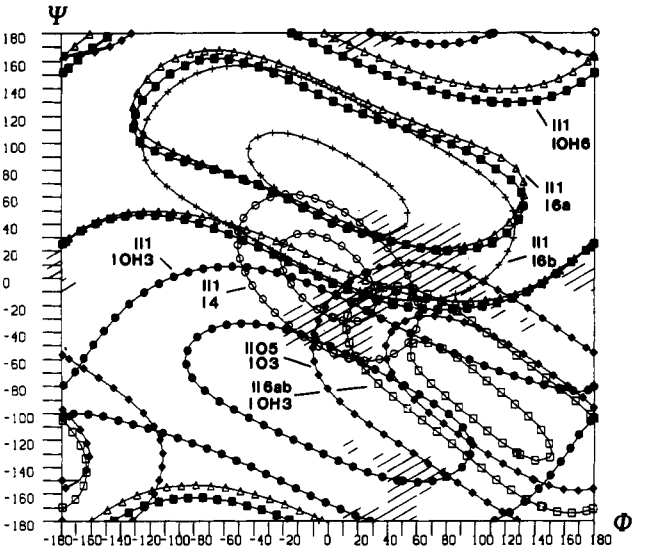

FIGURE 3: NOE, hydrogen bond (I3OH···O5II), and steric constraints for the Galβ1-4Glc linkage of the Neu4Ac5Gc-GM3 ganglioside (cf. Table IV). Labeling is as in Figure 1. Sterically allowed areas are hatched.

rather jumped immediately to values that corresponded to conformation 2 and then oscillated between those for conformations 2 and 1.

The conformational conduct of the side chain could be observed during all these simulations. As illustrated by the 1000-ps histories of the torsion angles shown in Figure 2d, the θ_1 and θ_2 angles remain practically constant, in accord with the rigidity of this segment of the side chain inferred from the experimental results discussed above. This is particularly important in view of the fact that four of the eight constraints demarcating the Neu-Gal linkage in each of the GM3 gangliosides were based on NOEs observed for H8. The changes of the H8-C8-C9-H9 torsion angle are of no importance in this respect. It should be noted that these changes were *not* synchronous with the jumps of the Φ,Ψ trajectories obtained *in the same calculation.* The H5-C5-N-H torsion angle oscillated around the experimentally assessed value of 180°, although with a larger scatter (simulation not shown).

Since solvation by water can be expected to affect the conformational behavior of saccharides, an aqueous environment was mimicked by the explicit inclusion of water molecules during a 350-ps simulation started with the geometry of conformation 1. As seen in Figure 2e, the Φ,Ψ trajectories oscillated synchronously between geometries 1 and 2, the latter occurring more frequently, however, than in a medium of low dielectric constant (Figure 2a). In contrast to the results obtained by Edge et al. (1990) for the Manα1-2Manα linkage, a dampening of torsional oscillations by water molecules was not observed. On the other hand, an even higher mobility in water than in nonpolar media has been reported for methoxytetrahydropyran (Grigera, 1990).

Conformation of Galβ1-4Glc Linkage. The constrains shown in Figure 3 demarcate two possible conformations with the Φ,Ψ angles at about (1) 55°,–5° and (2) –15°,–45° [MM2-85 minimized at (1) 51°,1°, and (2) 5°,–49°]. One of these constraints refers to the I3OH···O5II hydrogen bond, whose existence was inferred from the small coupling constant and temperature-shift coefficient for the IOH3 proton and is supported by similar findings concerning several glycolipids (Poppe et al., 1990a,b; Acquotti et al., 1990). Conformation 1 is practically identical with that considered to be the sole conformation of GM1 and GD1a (Sabesan et al., 1984, 1991b)

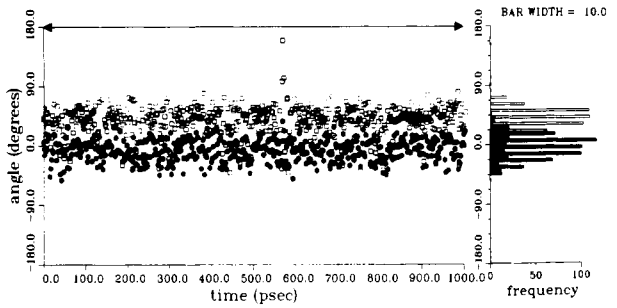

FIGURE 4: Histories of the glycosidic angles $\Phi(\square)$ and $\Psi(\bullet)$ for the Galβ1-4Glcβ disaccharide segment in a medium of $\epsilon = 8$; a 1000-ps simulation started with input values $\Phi = 51°, \Psi = 1°$.

and does not differ much, save the slightly different Ψ angle, from a total of 17 conformations calculated for GM1, GM1b, and GD1a (Scarsdale et al., 1990) ($\Phi = 40 \div 52°$; $\Psi = -15 \div -31°$). Conformations 1 and 2 match two of the three low-energy conformations found for GM3 by Veluraja and Rao (1983) (53°,4°; 16°,–41°; –12°,–29°) and two of the four conformations of GM1 recently described (Acquotti et al., 1990) (55°,0°; 5°,–30°; 35°,–50°; 170°,–5°). However, a MD simulation failed to reproduce transitions between discrete conformations with lifetimes comparable to those observed for the Neu5Acα2-3Gal linkage (Figure 4). Instead, the molecule sampled Φ,Ψ values within a large diapason, which roughly embraced the combinations corresponding to conformations 1 and 2 and the third conformation found for GM1 by Acquotti et al. (1990). Again, an exact correspondence is not expected since, as pointed out by Rasmussen and Fabricius (1990), a minimum in a two-dimensional conformational map may represent an entire family of points in multidimensional space; therefore, a "difference in Φ,Ψ of 10°,10° is really no difference at all". It seems that this linkage is very flexible and the barriers between the local minima are very low, so that it is more correct to speak of fluctuations within an extended energy valley rather than transitions between distinct conformers. A similar situation was described for globo and isoglobotriaosylceramides (Poppe et al., 1990a). A short excursion to $\Phi \approx 170°$ is the only indication of the possible occurrence of the fourth conformation described by Acquotti et al. (1990).

Conformation of Micelle-Bound GM3 Gangliosides and Their Mobility. The ganglioside–phosphatidylcholine mixed micelles showed narrow signals for protons of both the sugar and the ceramide moieties. The spectra shown in Figure 5 and the data presented in Tables VII and VIII refer to a GM3:DPC molar ratio of 1:40, but spectra of comparable quality were also obtained with a 1:20 ratio. In spite of the smaller number of NOE interactions observed for these deuterated samples, the N3ax/II3 contact referring to the Neu-Gal conformation 1, and the N8/II1 and N8/II3 contacts indicative of conformation 2, suggests that this linkage has a similar flexibility in both Me_2SO and in mixed micelles dissolved in D_2O (cf. Figure 1). In the case of Neu4Ac5Gc-GM3, the important N3ax/II3 cross-peak overlapped with the N3ax/N5 peak (Figure 5A,B) at all temperatures within a reasonable range. It was possible, however, to detect the spatial proximity of the N3ax and II3 protons with the aid of a selective 1D TORO measurement (for details, see Figure 5C).

The correlation times, τ_c, for GM3 in the mixed micelles and in the Me_2SO solution were estimated on the basis of the longitudinal relaxation time, T_{1_ρ}, for the N3ax proton in the rotating frame. The exponential fit of the data shown in Figure

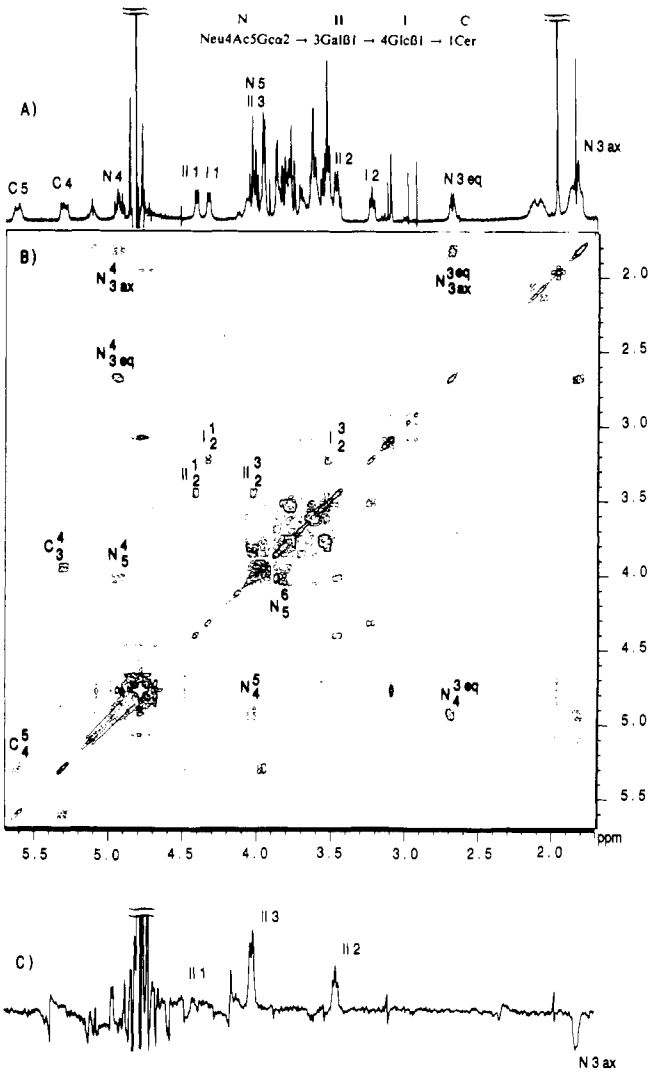

FIGURE 5: ^1H NMR spectra (500 MHz) of the micelle-bound Neu4Ac5Gc-GM3 ganglioside. Arabic numerals refer to protons in the C, I, II, and N moieties, labeled as shown in the formula. (A): Resolution-enhanced 1D spectrum. (B): $^1H/^1H$ autocorrelated (COSY) spectrum. For each cross-peak, the horizontal (F_2) and vertical (F_1) axes give the chemical shifts of the protons designated by the superscript and subscript, respectively. (C): A hybrid TOCSY–ROESY (TORO) spectrum obtained with selective excitation of the II1 proton. In the TOCSY step, magnetization is transferred in a coherent manner through bonds via II2 to II3, and in the following ROESY step it is incoherently transferred through space to the closely located N3ax proton, whose signal appears in the opposite phase.

6 gives $T_{1_\rho} = 0.26$ s in Me_2SO-d_6 and $T_{1_\rho} = 0.25$ s in D_2O/DPC-d_{38}, from which the corresponding cross relaxation rates, σ_{RF}, can be derived according to the relation $T_{1_\rho} = (2\sigma_{RF})^{-1}$ (Neuhaus & Williamson, 1989). With a sufficiently strong spin-locking field, $\sigma_{RF} \approx \sigma_\perp$ (Davis, 1987), correlation times can then be calculated with the following equation

$$(\sigma_\perp)_{ij} = (\gamma^4 h^2/40\pi^2 r_{ij}^6)[3/(1 + \omega_0\tau_c^2) + 2]\tau_c$$

where $\sigma_\perp$ is the transverse relaxation rate, γ is the magnetogyric ratio, h is Planck constant, and ω_0 is the Larmor frequency. Using the crystal data NH3ax/N3eq distance $r_{ij} = 1.78$ Å gives $\tau_c = 0.50 \cdot 10^{-9}$ s in Me_2SO and $0.53 \cdot 10^{-9}$ s in D_2O/DPC, i.e., the mobility of GM3 is roughly the same in both media. Moreover, since τ_c for a micelle of this size ($\sim$50 kDa) can be estimated with the well-known Debye formula, $\tau_c = 4\pi\eta r^3/3kT$ (where r is the radius of a spherical micelle, η is the viscosity of solution, k is the Boltzmann constant, and T is the temperature), to be of the order of 10^{-7} s, the above

Table VII: Chemical Shifts (ppm from Me_4Si) Measured at 500 MHz for Solutions of GM3 Gangliosides in D_2O/DPC at 303 K

residue	proton	Neu5Ac-GM3	Neu5Gc-GM3	Neu4Ac5Gc-GM3
Neuα-N	3ax	1.75	1.78	1.80
	3eq	2.71	2.69	2.66
	4	3.62	3.72	4.92
	5	3.78	3.84	3.99
	6	3.60	3.68	3.78
	7	3.55	3.52	3.48
	8	3.80	3.81	3.75
	9a	3.58	3.57	3.56
	9b	3.80	3.81	3.75
	10a		3.96	3.90
	10b		3.96	3.90
	NAc	1.97		
	OAc			1.98
Galβ-II	1	4.42	4.42	4.40
	2	3.46	3.46	3.46
	3	4.04	4.04	4.03
	4	3.88	3.90	3.88
	5	3.64	3.64	3.63
	6a	3.55	3.55	3.53
	6b	3.55	3.55	3.53
Glcβ-I	1	4.36	4.36	4.34
	2	3.26	3.27	3.25
	3	3.50	3.50	3.49
	4	3.55	3.55	3.54
	5	3.55	3.53	3.52
	6a	3.73	3.70	3.72
	6b	3.90	3.88	3.88
Cer-C[b]	1a	3.65	3.63	3.64
	1b	4.11	4.09	4.10
	2	3.81	3.83	3.80
	3	3.96	3.94	3.95
	4	5.38	5.35	5.36
	5	5.69	5.65	5.68

Table VIII: Interresidual Contacts and Corresponding NOE Distances, r_{kl}*, for the GM3 Gangliosides in D_2O/DPC

contacts		r_{kl}*	contacts		r_{kl}*
Neu5Acα2 → 3Galβ1 → 4Glc					
N3ax	II3	2.8	II1	I4	2.3
N8	II1	3.3	II1	I6a	3.2
Neu5Gcα2 → 3Galβ1 → 4Glc					
N3ax	II3	2.8	II1	I4	2.3
N8	II1	3.3	II1	I6a	3.2
N8	II3	2.9			
Neu4Ac5Gcα2 → 3Galβ1 → 4Glc					
N3ax	II3	*a*	II1	I4	2.3
N8	II1	3.2	II1	I6a	3.2
N8	II3	2.9			

[a] Because of signal overlap this contact was measured with the aid of a TORO experiment (Figure 5C) and hence could not be evaluated quantitatively.

result shows that at least the sugar moiety of GM3 retains its mobility within the micelle. It should be noted that the value of $\tau_c = 0.53$ ns compares well with 0.4 ns for a micelle-bound globoside, a value found by measuring relaxation rates at different magnetic fields (Poppe et al., 1990b), and also with a value of 0.5 ns obtained for the oligosaccharide of the GD1a ganglioside on the basis of carbon spin-lattice relaxation times (Sabesan et al., 1991b).

Conformation of Sialyllactoses in D_2O. The assignments for Neu5Ac-SL are in full agreement with those reported by Lerner and Bax (1987), and chemical shifts for Neu5Gc-SL and Neu5,9Ac_2-SL are almost identical, except for the understandable low-field shift of the N8,9a,9b resonances of the 9-*O*-acetylated derivative (Table IX).

For each of the sialyllactoses, two NOEs (N3ax/II3 and N8/II4) are the same as those that described Neu-Gal

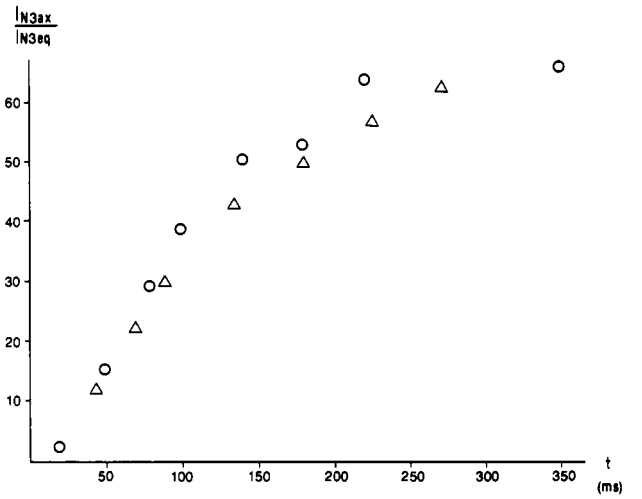

FIGURE 6: Rotating-frame NOE buildup for the N3ax protons of Neu4Ac5Gc-GM3 measured in DMSO-d_6 (△) and D_2O/DPC-d_{38} mixed micelles (○) and expressed as a percentage of the initial intensity of the N3eq signal, which was inverted by a DANTE pulse. Correlation coefficients are 0.990 and 0.992, respectively.

Table IX: Chemical Shifts (ppm from Me_4Si) Measured at 500 MHz for Solutions of Sialyllactoses in D_2O at 303 K

residue	proton	Neu5Ac-SL[a]	Neu5Gc-SL	Neu5,9Ac_2-SL
Neuα-N	3ax	1.81	1.82	1.84
	3eq	2.77	2.78	2.80
	4	3.70	3.77	3.71
	5	3.86	3.94	3.90
	6	3.65	3.76	3.69
	7	3.60	3.59	3.66
	8	3.90	3.90	4.12
	9a	3.68	3.67	4.20
	9b	3.90	3.90	4.48
	10a		4.15	
	10b		4.15	
	NAc	2.10		
	OAc			2.15
Galβ-II	1	4.56	4.53	4.53
	2	3.60	3.59	3.58
	3	4.14	4.13	4.13
	4	3.97	3.98	3.99
	5	3.72	3.69	3.71
	6a	3.80	3.83	3.80
	6b	3.80	3.83	3.80
Glcβ-I	1	4.68	4.67	4.68
	2	3.30	3.31	3.30
	3	3.64	3.63	3.63
	4	3.65	3.64	3.64
	5	3.62	3.62	3.62
	6a	3.85	3.83	3.80
	6b	3.98	3.97	3.96

[a] The values of Neu5Ac-SL are in accordance with those reported by Lerner and Bax (1987).

conformation 1, and two others (N8/II1 and N8/II3) refer to conformation 2 of this linkage (Table X; cf. Figures 1 and 7). It can therefore be concluded that the ceramide does not noticeably affect the conformation of this part of the sugar chain.

CONCLUSIONS

The spatial structure of a family of GM3 gangliosides was probed with the aid of rotating-frame NOEs obtained for C-, O-, and N-linked protons in Me_2SO solutions. Both the Neu-Gal and Gal-Glc glycosidic linkages showed a marked flexibility, confirmed by MD simulations, whereas the sialic acid side chains and the acylamino groups appeared to be fixed in one conformation. No appreciable conformational

Table X: Interresidual Contacts and Corresponding NOE Distances, r_{kl}*, for Sialyllactoses in D_2O

contacts		r_{kl}*	contacts		r_{kl}*
		Neu5Acα2 → 3Galβ1 → 4Glc			
N3ax	II3	2.9	II1	I4	2.3
N8	II1	3.2	II1	I6a	3.2
N8	II3	2.9	II1	I6b	3.0
N8	II4	3.3			
		Neu5Gcα2 → 3Galβ1 → 4Glc			
N3ax	II3	2.8	II1	I4	2.3
N8	II1	3.3	II1	I6a	3.2
N8	II3	2.9	II1	I6b	3.0
N8	II4	3.3			
		Neu5,9Acα2 → 3Galβ1 → 4Glc			
N3ax	II3	2.7	II1	I4	2.3
N8	II1	3.2	II1	I6a	3.2
N8	II3	2.9	II1	I6b	3.0
N8	II4	3.2			

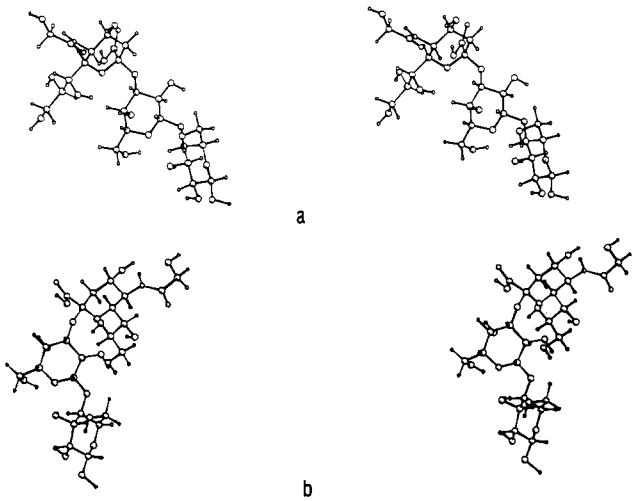

FIGURE 7: Stereodiagrams of two conformers of the sugar part of Neu5Gc-GM3 obtained from distance mapping (cf. Figures 1 and 3) followed by MM2 energy minimization of the whole trisaccharide. The Φ,Ψ angles for the Neu5Gcα2-3Galβ linkage are −160°, −24° in (a) and −73°,17° in (b), the Galβ1-4Glcβ linkage is in the 51°,1° conformation in (a) and 50°,2° in (b).

differences between 5Ac-, 5Gc-, 4Ac5Gc-, and 5,9Ac_2-substituted analogs were found for the glycosidic linkages, while slight deviations among the vicinal coupling constants (Tables II and III) suggested minor, probably insignificant differences in the orientation of the side chain and the amino moieties. It is concluded that the differences in the biological activity of these gangliosides, e.g., concerning their susceptibility to sialidases (Corfield & Schauer, 1982), can be accounted for by a direct interaction of the different acyl substituents with these enzymes, rather than by differing conformations of the sialic acid residues or the whole oligosaccharide moieties. It should be borne in mind, however, that all NMR-derived information concerning fast equilibria refers to average values of the corresponding structural parameters; hence, the above analysis does not exclude the existence of other, undetected conformations, which might be responsible for the interaction with enzyme receptors.

Although a considerably smaller number of NOE contacts were obtained for the GM3 gangliosides anchored in mixed DPC/D_2O micelles, the conformations seem to be similar to those in Me_2SO. Since the same applies to aqueous solutions of the corresponding free sialyllactoses, it can be concluded that the ceramide part does not appreciably affect the conformation of the oligosaccharide moieties.

REFERENCES

Acquotti, D., Poppe, L., Dabrowski, J., Lieth, C.-W. v. d., Sonnino, S., & Tettamanti, G. (1990) *J. Am. Chem. Soc. 112*, 7772–7778.

Bax, A., & Davis, D. G. (1985) *J. Magn. Reson. 65*, 355–360.

Bechtel, B., Wand, A. J., Wroblewski, K., Koprowski, H., & Thurin, J. (1990) *J. Biol. Chem. 265*, 2028–2037.

Breg, J., Kroon-Batenburg, L. M. J., Strecker, G., Montreuil, J., & Vliegenthart, J. F. G. (1989) *Eur. J. Biochem. 178*, 727–739.

Brisson, J.-R., & Carver, J. P. (1983) *Biochemistry 22*, 1362–1368.

Burkert, U., & Allinger, N. L. (1982) *Molecular Mechanics*, ACS Monograph 177, American Chemical Society, Washington, DC. See also Quantum Chemistry Program Exchange, Department of Chemistry, Indiana University, Bloomington, IN 47405, Program MM2<85>.

Bush, C. A., Yan, Z. Y., & Rao, B. N. N. (1986) *J. Am. Chem. Soc. 108*, 6168–6173.

Cantor, C. R., & Schimmel, P. R. (1980) *Biophysical Chemistry*, pp 253–260, H. Freeman & Co., San Francisco.

Corfield, A. P., & Schauer, R. (1982) *Cell Biol. Monogr. 10*, 195–261.

Dabrowski, J. (1989) *Methods Enzymol. 179*, 122–156.

Dabrowski, J., & Poppe, L. (1989) *J. Am. Chem. Soc. 111*, 629–630.

Dabrowski, J., Poppe, L., Siebert, H. C., & Lieth, C.-W. v. d. (1990) *Europhysics Conference Abstracts, Vol. 14H, Structure and Conformational Dynamics of Biomacromolecules* (Bethge, K., Ed.) p 45, European Physical Society, High Tatras.

Davis, D. G. (1987) *J. Am. Chem. Soc. 109*, 3471–3472.

Davis, D. G. (1989) *J. Magn. Res. 81*, 603–607.

de Vlieg, J., & van Gunsteren, W. F. (1991) *Methods Enzymol. 202*, 268–300.

Dezheng, Z., Toshimichi, F., & Nagayama, K. (1989) *J. Magn. Reson. 87*, 628–630.

Eaton, H. L., & Hakomori, S. (1988) *Third Chemical Congress of North America*, Abstract CARB 91, Toronto.

Edge, C. J., Singh, U. C., Bazzo, R., Taylor, G. L., Dwek, R. A., & Rademacher, T. W. (1990) *Biochemistry 29*, 1971–1974.

Eich, G., Bodenhausen, G., & Ernst, R. R. (1982) *J. Am. Chem. Soc. 104*, 3731–3732.

French, A. D. (1988) *Biopolymers 27*, 1519–1529.

French, A. D., & Brady, J. W. (1990) *Computer Modeling of Carbohydrate Molecules*, ACS Symposium Series 430, American Chemical Society, Washington, DC.

Grigera, J. R. (1990) in *Computer Modeling of Carbohydrate Molecules* (French, A. D., & Brady, J. W., Eds.) ACS Symposium Series 430, pp 152–161, American Chemical Society, Washington, DC.

Haasnot, C. A. G., de Leeuw, F. A. A. M., & Altona, C. (1980) *Tetrahedron 36*, 2783–2790.

Hagler, A. T., Huler, E., & Lifson, S. (1974) *J. Am. Chem. Soc. 96*, 5319–5327.

Hagler, A. T., Lifson, S., & Dauber, P. (1979) *J. Am. Chem. Soc. 101*, 5122–5130.

Hakomori, S.-I. (1990) *J. Biol. Chem. 265*, 18713–18716.

Higashi, H., Hirabayashi, Y., Fukui, Y., Naiki, M., Matsumoto, M., Ueda, S., & Kato, S. (1985) *Cancer Res. 45*, 3796–3802.

Homans, S. W., Dwek, R. A., Fernandes, D. L., & Rademacher, T. W. (1982) *FEBS Lett. 150*, 503–506.

Karplus, M., & McCammon, J. A. (1981) *CRC Crit. Rev. Biochem. 9*, 293–349.

Koerner, T. A. W., Prestegard, J. H., Demou, P. C., & Yu, R. K. (1983) *Biochemistry 22*, 2676–2687.

Koerner, T. A. W., Scarsdale, J. N., Prestegard, J. H., & Yu, R. K. (1984) *J. Carbohydr. Chem. 3*, 565–580.

Kessler, H., Griesinger, C., Kerssebaum, R., Wagner, K., & Ernst, R. R. (1987) *J. Am. Chem. Soc. 109*, 607–609.

Lemieux, R. U., Bock, K., Delbaere, L. T. J., Koto, S., & Rao, V. S. (1980) *Can. J. Chem. 58*, 631–653.
Lerner, L., & Bax, A. (1987) *Carbohydr. Res. 166*, 35–46.
Lieth, C.-W. v. d., Schmitz, M., Poppe, L., Hauck, M., & Dabrowski, J. (1989) in *Software-Entwicklung in der Chemie 3* (Gauglitz, G., Ed.) pp 371–378, Springer, Berlin.
Liliefors, M. (1983) *J. Mol. Graphics 1*, 111–117.
Lipkind, G. M., Shashkov, A. S., Nechaev, O. A., Torgov, V. I., Shibaev, V. N., & Kochetkov, N. K. (1989) *Carbohydr. Res. 195*, 11–25 and 27–37.
Marion, D., & Wüthrich, K. (1983) *Biochem. Biophys. Res. Commun. 113*, 967–974.
Marion, D., & Bax, A. (1988) *J. Magn. Reson. 79*, 352–356.
Michon, F., Brisson, J.-R., & Jennings, H. J. (1987) *Can. J. Chem. 26*, 8399–8405.
Müller, L., & Ernst, R. R. (1980) *Mol. Phys. 38*, 963–992.
Neuhaus, D., & Williamson, M. P. (1989) *The Nuclear Overhauser Effekt in Structural and Conformational Analysis*, VCH Publishers, New York.
Noggle, J. H., & Schirmer, R. E. (1971) *Nuclear Overhauser Effect*, Academic Press, New York.
Ogura, H., Furuhata, K., Sato, S., Anazawa, K., Itoh, M., & Shitori, M. (1987) *Carbohydr. Res. 167*, 77–86.
Paulsen, H., Peters, T., Sinnwell, V., Lebuhn, R., & Meyer, B. (1984) *Liebigs Ann. Chem.*, 951–976.
Peters, T., Brisson, J.-R., & Bundle, D. R. (1990) *Can. J. Chem. 68*, 979–988.
Piantini, U., Sorensen, O. W., & Ernst, R. R. (1982) *J. Am. Chem. Soc. 104*, 6800–6801.
Poppe, L., & Dabrowski, J. (1989) *Biochem. Biophys. Res. Commun. 159*, 618–623.
Poppe, L., Dabrowski, J., Lieth, C.-W. v. d., Koike, K., & Ogawa, T. (1990a) *Eur. J. Biochem. 189*, 313–325.
Poppe, L., Lieth, C.-W. v. d., & Dabrowski, J. (1990b) *J. Am. Chem. Soc. 112*, 7762–7771.
Rance, M. (1987) *J. Magn. Reson. 74*, 557–564.
Rasmussen, K., & Fabricius, J. (1990) in *Computer Modeling of Carbohydrate Molecules* (French, A. D., & Brady, J. W., Eds.) ACS Symposium Series 430, pp 177–190, American Chemical Society, Washington, DC.
Reuter, G., & Schauer, R. (1987) in *Gangliosides and Modulation of Neuronal Functions* (Rahmann, H., Ed.) NATO ASI Series H: Cell Biology, Vol. 7, pp 155–167, Springer Verlag, Berlin, Heidelberg, and New York.
Sabesan, S., Bock, K., & Paulson, J. C. (1991a) *Carbohydr. Res. 218*, 27–54.
Sabesan, S., Duus, J. O., Fukunaga, T., Bock, K., & Ludvigsen, S. (1991b) *J. Am. Chem. Soc. 113*, 3236–3246.
Scarsdale, J. N., Prestegard, J. H., & Yu, R. K. (1990) *Biochemistry 29*, 9843–9855.
Schauer, R. (1979) *Methods Enzymol. 50*, 374–386.
Sorensen, O. W., Rance, M., & Ernst, R. R. (1984) *J. Magn. Reson. 56*, 527–534.
Subramanian, S., & Bax, A. (1987) *J. Magn. Reson 71*, 325–330.
Taravel, F. R., & Vignon, M. R. (1982) *Polymer Bull. 7*, 153–157.
Tran, V., Bouleou, A., & Perez, S. (1989) *Biopolymers 28*, 679–690.
Tvaroska, I., & Perez, S. (1986) *Carbohydr. Res. 149*, 389–410.
Veh, R. W., Sander, M., Haverkamp, J., & Schauer, R. (1979) *Proceedings of the Fourth International Symposium on Glycoconjugates*, pp 557–559, Academic Press, New York.
Veluraja, K., & Rao, V. S. R. (1983) *Carbohydr. Polym. 3*, 175–192.
Wiegandt, H., & Bücking, H. W. (1970) *Eur. J. Biochem. 15*, 287–292.